International Journal of Mechatronics and Applied Mechanics
2025, Issue 19, Vol. 1

KINEMATICS ANALYSIS AND SIMULATION OF LASER WELDING ROBOT FOR SOLAR PANEL BUSBAR

Wang Peng[1,2], Zheng Mingliang[1,2,] [0000-0001-5681-0051]*
[1]School of Mechanical and Electrical Engineering, Huainan Normal University, Huainan 232038, China
[2]Human-computer collaborative robot Joint Laboratory of Anhui Province, Huainan 232038, China
Email: liangmingzheng@hnnu.edu.cn

Abstract - To overcome the insufficient quality stability of the overlap welding joints of solar panel busbar, using laser brazing technology, a new type of serial gantry robot with five degrees of freedom (three translations and two rotations) is designed. Firstly, the structure scheme of the gantry laser welding robot with five degrees of freedom for solar panel busbar is introduced. Secondly, the D-H linkage coordinate system of the welding robot is established, and the kinematics forward and inverse solutions and the velocity Jacobian matrix are solved. Finally, the kinematics forward and inverse solutions are verified by using Robotics toolbox in Matlab; the reachable space of the robot is calculated by Monte-Carlo method; the kinematics simulation of the laser welding robot end effector is carried out by using Adams software. The results show that the displacement of the end effector of the gantry laser welding robot with five degrees of freedom for solar panel busbar is non-interference and the velocity curves change smoothly, which verifies the rationality of this structural design. By making a prototype and building a test platform for experimental verification, the robot ran smoothly, the weld seam layout was efficient and accurate, and the error at the end of the robot welding gun was within 0.28 mm.

Keywords: Solar panel busbar, Laser welding, Kinematic forward and inverse solutions, Matlab Robotics, Adams simulation.

1. Introduction

Busbar welding is a crucial process in the production of solar panel modules, and its welding performance directly determines the working efficiency of the solar panel [1-2]. Among them, because laser welding can be used for non-contact welding, it has the advantages of high energy density, high ratio of penetration deep to weld width, fast welding speed, good repeatability, small workpiece deformation, and small heat affected area [3-4], therefore, laser welding of solar panel busbar will have a broad application prospect in the world photovoltaic power generation industry. Laser welding of solar panel busbar is to weld the interconnection belts on two adjacent battery strings together to play the role of parallel battery strings. At present, the equipment for solar panel busbar welding in domestic and foreign markets is not sufficient, and the welding quality and efficiency of traditional laser welding machines are difficult to meet the requirements. In order to improve the welding quality and efficiency of solar panel busbar, a gantry type automatic laser welding robot is designed and studied in this paper.

With the introduction of concepts such as Industry 4.0, intelligent manufacturing has become a trend in industrial development, and welding robots are becoming increasingly diversified, intelligent, and flexible [5]. However, most welding robots are inconvenient to move and cannot weld continuously uniformly. Therefore, developing an intelligent robot for the welding task of solar panel busbar is of great significance for the development and improvement of intelligent welding technology in world. As a manifestation of industrial automation technology, automatic laser welding robots can automatically perform welding operations, so the motion trajectory of welding robots becomes one of the main factors affecting welding accuracy [6]. At present, 6-axis serial industrial robots are capable of performing a large number of welding operations, such as placing the industrial robot system on movable guide rails or gantry frames for workpieces with large dimensions and complex geometric shapes, adding 1-3 external axes, and equipped with 1-2 axis positioners, which can expand the working space of the industrial robot itself and achieve good connection positions between the workpiece

https://doi.org/10.17683/ijomam/issue19

connection parts and the industrial robot system. This article studies the combination of gantry mechanism and laser welding technology to construct an automatic laser welding robot. On the one hand, it can avoid machine tool errors caused by cutting forces, and on the other hand, it can apply the advantages of gantry mechanism to automatic laser welding, thereby enabling the serial robot to be better applied in the field of automatic welding.

The laser welding robot for solar panel busbar in this paper has five degrees of freedom x, y, z, R, R, so it has good mobile performance. In order to verify the feasibility of the structural design, the kinematics analysis and simulation of the laser welding robot for solar panel bus bar were carried out. Kinematics analysis of robots [5-10] is not only the basis of robot dynamics analysis, but also provides a basis for the research on robot motion space, motion control, trajectory planning. In this paper, the D-H linkage coordinate system [11] of the welding robot is established, and the analytical expressions of kinematic forward and inverse solutions [12-13] are obtained by algebraic method. Then, the kinematic forward and inverse solutions are verified by using Robotics toolbox in Matlab. Secondly, Monte-Carlo method is used to display the motion space of the welding robot [14-15], which can intuitively reflect the motion space of the robot in three-dimensional space. Finally, we use Adams software to conduct kinematics simulation research on the end effector of the robot [16-17], and evaluate whether its motion characteristics are reasonable.

1.1 Structural Design of Solar Panel Busbar Laser Welding Robot

Through in-depth understanding of various gantry type machine tools and laser welding machines, comprehensively analyze the reliability and complexity of the mechanism, as well as the laser welding characteristics and process of solar panel busbar, meanwhile, according to the problems in the production of the traditional laser welding machine, taking into account the shape characteristics of the solar panel busbar overlay welding, and combining with the performance and technical requirements of the laser welding machine, we put forward the overall scheme of the equipment [18]. The overall scheme of laser welding robot is shown in Figure 1.

The mechanical structure of the equipment consists of five parts. The first part is the design of the lathe bed and X-axis. The X-axis linear motor drives the solar panel busbar (workpiece) clamp to move in the X-direction, and the lathe bed plays a supporting role to ensure the sufficient static and dynamic stiffness. The second part is the design of the upright column. The upright column is mainly used to support and meet the Z-direction movement of the laser welding head. Therefore, the upright column should have enough stiffness and the welding head should have enough height during the design, meanwhile, it is necessary to prevent the upright column from being too high, causing the entire lathe bed to overturn. The third part is the design of the Y-axis. The laser welding head is driven along the Y-axis direction by the Y-axis linear motor. The fourth part is the design of the Z-axis. The Z-axis servo motor and ball screw combine transmission to drive the laser welding head up and down and to focus the laser on the solar panel busbar (workpiece). The fifth part is the laser welding body. The body base is fixedly connected to the Z-axis beam, which has two rotation joints.

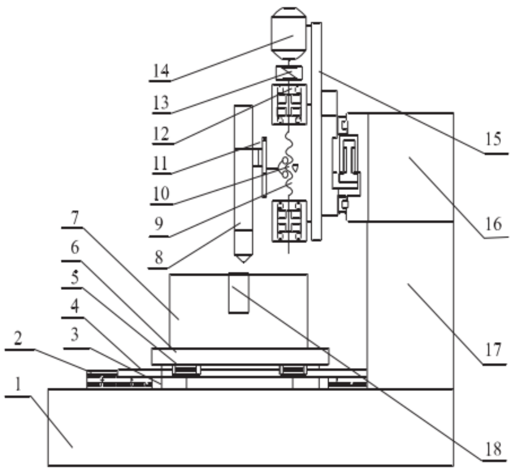

1—Marble lathe bed; 2—X-axis linear motor stator; 3—X-axis linear motor mover; 4—X-axis guide rail; 5—X-axis slider; 6—X-axis sliding plate; 7—Work-piece clamp; 8—Laser welding head; 9—Ball screw; 10—Screw nut; 11—Z-axis sliding plate; 12—Bearing and bearing components; 13—Coupling; 14—Z-axis servo motor; 15—Z-axis base; 16—Y-axis (linear motor module); 17—Marble upright column; 18—Solar panel busbar (workpiece).

Figure 1: Structural design of laser welding robot for solar panel busbar

The solar panel busbar laser welding robot system has a total of five degrees of freedom, that is, three linear moving pairs and two rotating pairs. The joint forms are shown in Figure 2.

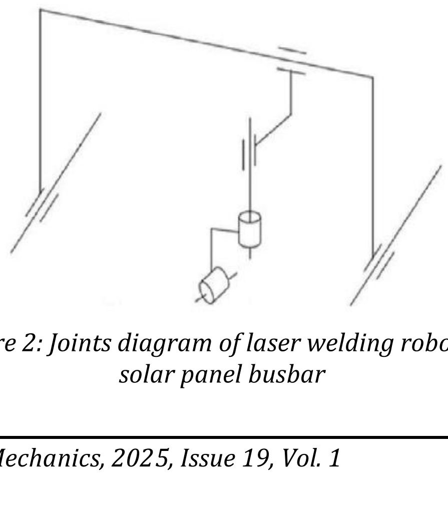

Figure 2: Joints diagram of laser welding robot for solar panel busbar

1.2 Calculation and analysis of critical speed

Kinematics of mechanism is a method to study how the joints of mechanism move. It includes two aspects: one is to solve the kinematic forward, the other is to solve the kinematic inverse. Kinematic forward means that the change angle and displacement of each joint of the mechanism are known, and the trajectory and attitude of the actuator at the end of the mechanism can be solved, significantly, the result is only one solution. Kinematic inverse refers to the inverse calculation of how each joint moves to achieve the attitude and position of the actuator at the end of the mechanism, significantly, the solution is often not unique.

Firstly, we analyze the D-H connecting rod parameters of the solar panel busbar laser welding robot, as shown in Table 1.

Table 1. D-H connecting rod parameters

i	α_{i-1}	d_i	a_{i-1}	θ_i
1	-pi/2	d_1	0	pi/2
2	pi/2	d_2	a_1	0
3	-pi/2	d_3	a_2	pi/2
4	0	d_4	0	θ_4
5	α_4	d_5	0	θ_5

According to the D-H coordinate method, the relationship between the end actuator and the base can be expressed as:

$$
\begin{aligned}
{}^0T_5 &= {}^0A_1\,{}^1A_2\,{}^2A_3\,{}^3A_4\,{}^4A_5 \\
&= \begin{bmatrix} 0 & -1 & 0 & 0 \\ 0 & 0 & 1 & d_1 \\ -1 & 0 & 0 & 0 \\ 0 & 0 & 0 & 1 \end{bmatrix}
\begin{bmatrix} 1 & 0 & 0 & a_1 \\ 0 & 0 & -1 & -d_2 \\ 0 & 1 & 0 & 0 \\ 0 & 0 & 0 & 1 \end{bmatrix} \\
&\quad \begin{bmatrix} 0 & -1 & 0 & a_2 \\ 0 & 0 & 1 & d_3 \\ -1 & 0 & 0 & 0 \\ 0 & 0 & 0 & 1 \end{bmatrix}
\begin{bmatrix} \cos\theta_4 & -\sin\theta_4 & 0 & 0 \\ \sin\theta_4 & \cos\theta_4 & 0 & 0 \\ 0 & 0 & 1 & d_4 \\ 0 & 0 & 0 & 1 \end{bmatrix} \\
&\quad \begin{bmatrix} \cos\theta_5 & -\sin\theta_5 & 0 & 0 \\ \sin\theta_5\cos\alpha_4 & \cos\theta_5\cos\alpha_4 & -\sin\alpha_4 & -d_5\sin\alpha_4 \\ \sin\theta_5\sin\alpha_4 & \cos\theta_5\sin\alpha_4 & \cos\alpha_4 & d_5\cos\alpha_4 \\ 0 & 0 & 0 & 1 \end{bmatrix} \\
&= \begin{bmatrix} n_x & o_x & w_x & p_x \\ n_y & o_y & w_y & p_y \\ n_z & o_z & w_z & p_z \\ 0 & 0 & 0 & 1 \end{bmatrix}
\end{aligned} \tag{1}
$$

Here, the vectors $\vec{n}, \vec{o}, \vec{w}$ respectively represent the attitude vectors in the end effector coordinate system, and the vector $\vec{p}$ represents the position vector in the reference coordinate system.

So the result of kinematic forward solution is:

$$
\begin{aligned}
n_x &= -\cos\theta_4\cos\theta_5 + \sin\theta_4\sin\theta_5\cos\alpha_4, \\
o_x &= \cos\theta_4\sin\theta_5 + \sin\theta_4\cos\theta_5\cos\alpha_4, \\
w_x &= -\sin\theta_4\sin\alpha_4, \\
p_x &= -d_5\sin\theta_4\sin\alpha_4 + d_2, \\
n_y &= \sin\theta_5\sin\alpha_4, \\
o_y &= \cos\theta_5\sin\alpha_4, \\
w_y &= \cos\alpha_4 + d_2, \\
p_y &= d_5\cos\alpha_4 + d_4 + d_3 + d_1, \\
n_z &= \sin\theta_4\cos\theta_5 + \cos\theta_4\sin\theta_5\cos\alpha_4, \\
o_z &= -\sin\theta_4\sin\theta_5 + \cos\theta_4\cos\theta_5\cos\alpha_4, \\
w_z &= -\cos\theta_4\sin\alpha_4, \\
p_z &= -d_5\cos\theta_4\sin\alpha_4 - a_2 - a_1.
\end{aligned} \tag{2}
$$

Next, we analyze the kinematic inverse solution. It is obvious that:

$$\theta_5 = \arctan\frac{n_y}{o_y} \tag{3}$$

Substituting equation (3) into equation (2) to get:

$$\theta_4 = -\arcsin\left(\frac{w_x}{n_y}\sin\theta_5\right) \tag{4}$$

After the θ_4 and θ_5 expressions are obtained, there may be more than one set of numerical results, and the final specific quadrant selection should be determined according to the continuity of motion. Substituting the θ_4 and θ_5 into equation (2) can obtain the specific expressions of other parameter $\alpha_4, a_1, a_2, d_1, d_2, d_3, d_4, d_5$ for kinematic inverse solution.

By using Jacobian matrix and its inverse matrix, the coordinate transformation of forward and inverse relative to the base for the angular velocity of each joint of the solar panel busbar laser welding robot can be obtained, and it can connect a certain joint of the laser welding robot with the whole. The Jacobian matrix can be expressed as:

$$J = \left[\frac{\partial\, {}^0T_5}{\partial\theta_4}, \frac{\partial\, {}^0T_5}{\partial\theta_5}\right] \tag{5}$$

1.3 Kinematic Simulation

1. Robotics modeling to verify the forward and inverse solutions

Using Robotics toolbox in Matlab to model the robot according to the D-H connecting rod parameters, and setting the initial position: $\alpha_4 = -\pi/3, \theta_4 = \pi/2, \theta_5 = -\pi/2, a_1 = a_2 = 0.15,$ $d_1 = 0, d_2 = -1, d_3 = 1, d_4 = -0.3408, d_5 = -2.556$. So the theoretical pose matrix of the tool coordinate system can be calculated by substituting the initial position into equation (1):

$$ {}^{0}T_5 = \begin{bmatrix} 0.5 & 0 & -0.866 & 1.214 \\ -0.866 & 0 & -0.5 & -0.6189 \\ 0 & 1 & 0 & -0.3 \\ 0 & 0 & 0 & 1 \end{bmatrix} \tag{6} $$

Figure 3 shows the modeling of the robot using Robotics toolbox, we can see the identified initial position. Further, using the fkine function in Matlab, we can get the value of the pose matrix, which is exactly the same as the equation (6), so the analytic expressions of kinematic forward and inverse solutions in section 2 are verified correct.

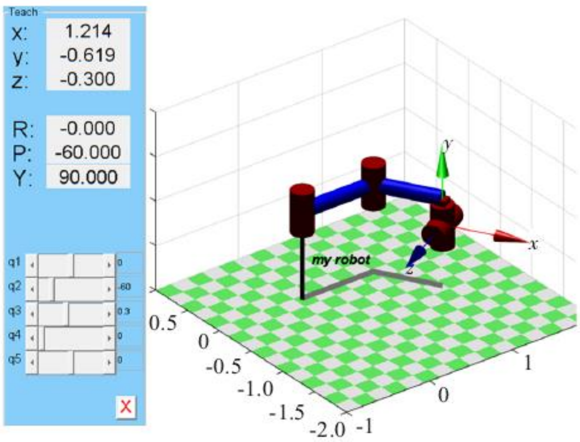

Figure 3: Robotics modeling

2. Workspace Simulation of end Effector of Laser Welding Robot

Before a welding robot is given a task, it is often necessary to know clearly the reachable workspace of the welding robot. In MATLAB, the Monte-Carlo method can be used to randomly sampling in the range of motion of each joint angle. Kinematic forward solutions for a large number of sample points are the corresponding positions of the end actuator. By drawing the corresponding positions of the end actuator, the robot workspace can be visualized. Setting the random number to 2000 times, so the workspace simulation of the robot end effector is shown in Figure 4.

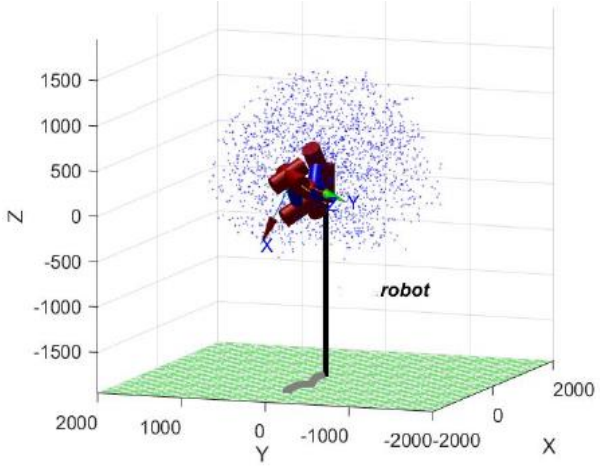

Figure 4: Robot motion space

The blue area in Figure 4 is the workspace of the robot. It can be seen from the three-dimensional simulation Figure 4 that the reachable boundary range of the solar panel busbar welding robot can meet the requirements of the actual welding area. Its movement space is -0.5~1.5m in the Z-direction, the maximum displacement of the X-direction can reach 3.5m, and the maximum displacement of the Y-direction can reach 2.5m, which conform to the space range limit of the welding action.

3. Kinematics simulation of the whole machine

Figure 5 shows the 3D solid model of the solar panel busbar laser welding machine established in SolidWorks software, which is imported into Adams software in the format of Parasolid. file for kinematics simulation.

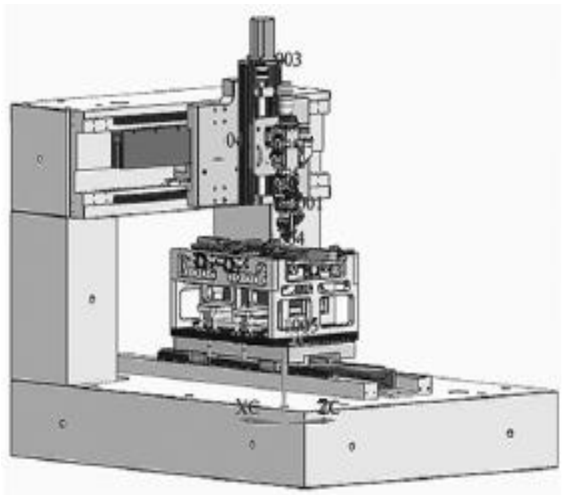

Figure 5: The model in Adams

Setting the displacement functions of the three prismatic joints and the velocity functions of the two rotation joints of the laser welding robot as:
X-axis: Step (time, 0, 0, 0.009, 2300) + Step (time, 0.3892, 0, 0.3894, -2300) + Step (time, 1.8346, 0, 1.8676, 2300) + Step (time, 1.9556, 0, 1.9886, -2300);

Y-axis: Step (time, 1.1924, 0, 1.2016, 2300) + Step (time, 1.8346, 0, 1.8674, -2300) + Step (time, 1.9556, 0, 1.9886, -2300) + Step (time, 2.4896, 0, 2.5226, 2300) + Step (time, 2.6436, 0, 2.6528, -2300) + Step (time, 2.7556, 0, 2.7846, 2300);
Z-axis screw: Step (time, 0.3984, 0, 0.4112, 1440) + Step (time, 1.1794, 0, 1.1924, -1440);
Z-axis screw nut: Step (time, 0.3984, 0, 0.4112, 64) + Step (time, 1.1794, 0, 1.1924, -64);
Rotation joint1: Step (time, 0, 0, 10, 5d) + Step (time, 15, 0, 20, -5d);
Rotation joint2: Step (time, 0, 0, 10, -5d) + Step (time, 15, 0, 20, 5d).
Here, Step is a step function, 5d is the rotational angular velocity of the simulated joint.

Curve A in Figure 6 is the displacement of the end effector of welding robot in X-direction, curve B is the displacement in Y-direction, and curve C is the displacement in Z-direction. It can be seen that the maximum displacement in the X-direction is 310cm, the maximum displacement in the Y-direction is 220cm, and the maximum displacement in the Z-direction is 130cm. The maximum limit values of X, Y and Z directions in the workspace of the welding robot are 350cm, 250cm and 150cm respectively, so the maximum displacement values of X, Y and Z directions in curves A, B and C are less than the limit values of the workspace, which shows there is no interference in the displacement of the mechanism, so the simulation results meet the requirements of the actual work of the robot.

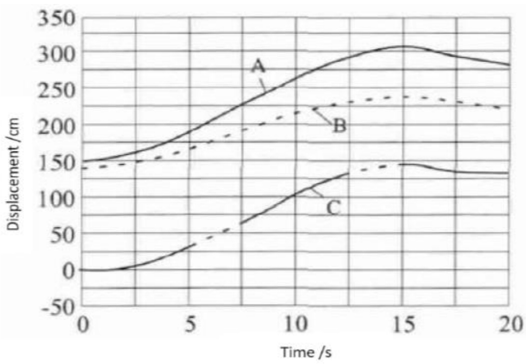

Figure 6: Displacement curves of the end of robot

From Figure 6, it can be seen that as the stiffness of the upper support increases along the order of magnitude, both the first and second critical speeds increase, and the second-order change rate is significantly larger. When the stiffness increases from 1.0×10^6 (N/m) to 1.0×10^8 (N/m), the second-order critical speed undergoes a step change and then tends to slow down. At this point, due to the excessive stiffness, it can be approximated as a fixed support, and the impact on the critical speed gradually reaches its upper limit.

Curve D in Figure 7 is the velocity of the end effector of welding robot in the X-direction, curve E in Figure 7 is the velocity in the Y-direction, and curve F in Figure 7 is the speed in the Z-direction. It can be seen that the velocity change of the end effector is -7~15.5 cm/s, while the fastest velocity of the welding head can reach 20 cm/s, so the welding velocity meets the requirements.

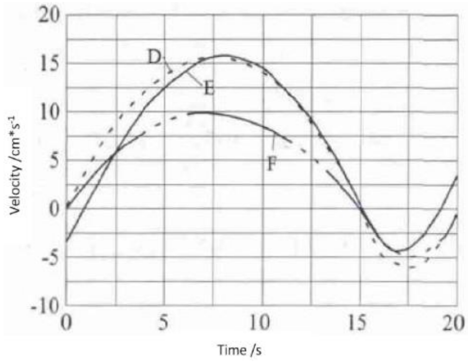

Figure 7: Velocity curves of the end of robot

In addition, it can be seen from the curves in Figure 6 and Figure 7 that with the welding movement of the laser welding robot, the curve changes in all directions are continuous and gentle, without mutation, which indicats that when the robot is welding, each mechanism component runs smoothly without severe impact, so the robot can ensure the smooth progress of the welding work.

1.4 Experimental Study

Using a robot platform, conduct laser welding experiments on solar panel busbar. Connecting the laser welding head at the end of the robot and using beam movement and specimen fixation for welding. Using manual feeding and clamping. The base metal of busbar is TU1 oxygen free copper sheet, its length, width and thickness are 600mm×100mm×0.35mm. The base metal of interconnection belt is also TU1 oxygen free copper sheet, its length, width and thickness are 200mm×40mm×0.15 mm, these base metals are both in rolled and annealed state. The brass solder is tin solder. The output power of the laser is 2.8 kW. The welding process is shown in Figure 8.

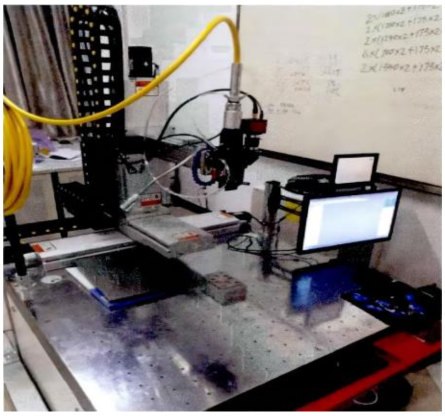

Figure 8: The process of robot laser welding

The welding test sample is shown in Figure 9, and it can be seen that the weld seam is flat, continuous, and uniform, which verifies the accuracy and continuity of the robot's motion.

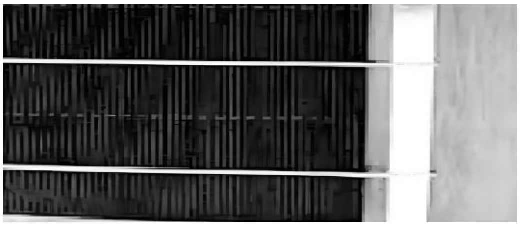

Figure 9: Busbar welding test

During the welding process, 10 sets of joint coordinate values are randomly collected by the upper computer and inputted into the forward kinematics expression, and compared with the robot end coordinate values to obtain the robot accuracy. As shown in Figure 10, the welding accuracy of the robot is within 0.28 mm, which meets the precision requirements of the welding robot.

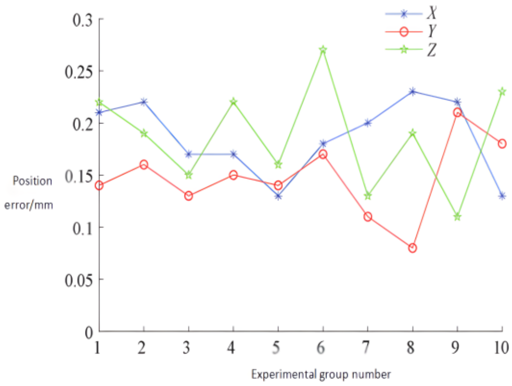

Figure 10: Robot motion accuracy error

2. Conclusions

In this paper, the mechanical structure and kinematics of the solar panel busbar laser welding robot are analyzed by combining theory with computer simulation. The main contents are as follows:

(1) A gantry type laser welding robot with five degrees of freedom for solar energy battery panel busbar is designed. The Z-axis linear module moves up and down to focus the laser, and the X/Y axes drive the laser welding head to move along the predetermined trajectory. The laser welding body has two rotary joints to realize the one-time overlap welding of the solar panel busbar and interconnection belt.

(2) The D-H parameter coordinate system of the welding robot is established, and its kinematic forward and inverse models are derived. The forward and inverse solutions are analytical solutions, which have the advantages of strong real-time and easy control.

(3) Under the Matlab simulation environment, with Robotics toolbox, the verified kinematic forward and inverse solutions of the solar panel busbar laser welding robot are obtained. Meanwhile, combining with the Monte-Carlo random number algorithm, the workspace of the welding robot during welding is simulated, so that the movement of the robot can be seen more intuitively.

(4) Conducting the motion simulation of the whole machine by Adams software, the displacement curve of the actuator at the end of the welding robot changes within the working space, and the whole machine will not have motion interference. The velocity curve changes continuously and gently, without mutation. which proves that there is no severe impact during welding. Therefore, the structure design meets the requirements.

(5) A robot prototype was made for welding tests, and the robot clamping was reliable. The surface morphology of the busbar welding was smooth and sturdy, and the absolute accuracy of the robot reached within 0.28mm.

Further, the trajectory planning of the welding robot can be studied. At the same time, the mechanical structure of the laser welding head can be changed to enable the welding robot to complete more complex operations in solar panel busbar laser welding.

Acknowledgements (Not Mandatory)

This research received a supported by Qing Lan Project of Universities in Jiangsu Province (2022-29).

References

[1] Biram, D., Jean P.T., Senghane M. (2020). Solar panels optimization for a better efficiency and for hot water production: Determination of the exchange coefficient. *International Journal of Engineering & Technology*, 12(3), 476-482.

[2] Skupov, A. A., Panteleev, M. D., Shcherbakov, A. V. (2022). Laser welding of fuselage panels from aluminum V-1579 and aluminum-lithium V-1481 alloys. *Welding Internationa*, 36(2), 92-96.

[3] You, D.Y., Gao, X.D. (2008). Studies and prospect of laser welding technology. *Welding Technology*, 37(4), 5-9.

[4] Krylova, S.E., Zavyalov, V.A., Goltapin, M.I. (2020). Development of Technology of Robotized Laser Welding of Thin Wall Products from Heat-Resistant Alloys. *Materials Science Forum*, 5952, 663-669.

[5] Polivanov, A. Y., Ivanov, Y. V., Kholin, D. V. (2020). The Method of the Computer Vision System Coordinate Transformation for an Industrial Robot for a Laser Welding Operation. *Mekhatronika, Avtomatizatsiya, Upravlenie,* 21(3), 166-173.

[6] Davide, M. B., Lorenzo M. T., Barbara P., Ali Gökhan D. (2024). Seam tracking and gap bridging during robotic laser beam welding via grayscale imaging and wobbling, 89: 102774.
[7] Zhang, W. J., Zou, J., Watson, L. G. (2002). The constant-Jacobian method for kinematics of a three-DOF planar micro-motion stage. *Journal of Robotic Systems*, 19(2), 63-72.
[8] Huang, Z., Zhao, Y.S., Zhao, T.S. (2006). *Advanced spatial mechanism*. Beijing: Higher Education Press.
[9] Jia, Y.H., Misra, A. K. (2018). Trajectory planning for a space robot actuated by control moment gyroscopes. *Journal of Guidance, Control and Dynamics*, 41(8), 1833-1841.
[10] Asif, S., Webb, P. (2021). Kinematics Analysis of 6-DoF Articulated Robot with Spherical Wrist. *Mathematical Problems in Engineering*, 1, 6647035.
[11] Chen, H.T., Ma, H.J., Jiang, H.L. (2022). Kinematic Modeling of 3P2R Welding Robot Based on D-H Parameters. *Journal of Physics: Conference Series*, 2218(1), 012085.
[12] Jiang, Y., Han, Q.Q., Dai, Z.E. (2022). Structural design and kinematic analysis of a welding robot for liquefied natural gas membrane tank automatic welding. *The International Journal of Advanced Manufacturing Technology*, 122(1), 461-474.
[13] Oliveira, L.F.P.D., Flávio, L.R. (2018). Modeling, simulation and analysis of locomotion patterns for hexapod robots. I*EEE Latin America Transactions*, 16(2), 375-383.
[14] Sivasamy, D., Anand, M.D., Sheela, K.A. (2019). Robot Forward and Inverse Kinematics Research using Matlab. *International Journal of Recent Technology and Engineering*, 8(2), 29-35.
[15] Nikolaos, K., Emmanouil, O., Michail, G.L. (2015). Complete Analytical Forward and Inverse Kinematics for the NAO Humanoid Robot. *Journal of Intelligent & Robotic Systems*, 77(2), 251-264.
[16] Nguyen, Q. V., Colas, F., Vincent, E. (2017). Long-term robot motion planning for active sound source localization with Monte Carlo tree search. *Hands-free Speech Communications & Microphone Arrays* (pp. 25-30). IEEE.
[17] Qu, M., Wang, H., Rong, Y. (2017). Design of 6-DOF parallel mechanical leg of wheel-leg hybrid quadruped robot. *Transactions of the Chinese Society of Agricultural Engineering*, 33(11), 29-37.
[18] Zhe, X., Jun, Y.G. (2014). The Kinematics and Dynamics Analysis of Rescue Robot Based on Adams and Matlab Simulation. *Advanced Materials Research*, 3227(945), 1400-1407.
[19] Lu, Z.G., Qi, X.F., Wang, H. (2013). Co-simulation System for A Humanoid Robot Based on Pro/E ADAMS and MATLAB. *Information Technology Journal*, 12(19), 5238-5244.
[20] Bai, Y.T. (2020). Design and analysis of mechanical system for automatic welding production line of solar panel busbar. Ningxia: Ningxia University.